

An investigation of grain-boundary plane crystallography in polycrystalline nickel

V. RANDLE

Department of Materials Engineering, University College of Swansea, Swansea SA2 8PP, UK

An investigation has been carried out to measure and categorize the grain-boundary plane indices of boundaries in pure nickel. Coincidence site lattices (excluding $\Sigma = 3$ s) were found to be either asymmetrical tilt boundaries with high indices, or have irrational boundary planes. For the $\Sigma = 3$ s, almost half were asymmetrical tilt boundaries displaced from the $111/111$ symmetrical tilt boundary on the 110 zone. Such boundaries have low energies compared to other $\Sigma = 3$ s. The $211/211$ incoherent twin was not observed, which was explained on the basis of its higher energy compared to other boundaries on the 110 zone. The results are compared and contrasted with previous data, where boundaries abutted the specimen surface during annealing, which is not the case for the present data. Comments are made with respect to the relationship between macroscopic and atomic-level boundary geometry and implications of the results for grain-boundary properties.

1. Introduction

Annealing twins, i.e. $\Sigma = 3$ boundaries in coincidence site lattice (CSL) notation, are ubiquitous in low stacking fault energy face-centred cubic materials. Twins can often be inferred in the microstructure from their straight morphology. However, unambiguous classification requires a knowledge of the lattice misorientation between neighbouring grains, because a $\Sigma = 3$ interface is characterized by a rotation of 60° about a 111 axis. Misorientations are calculated from grain-orientation measurements made using electron back-scatter diffraction (EBSD) in a scanning electron microscope (or other techniques), which allows not only twins to be recognized but also other misorientation types, such as CSLs or low-angle boundaries [1, 2]. Obtaining lattice orientations and misorientations using EBSD is now routine; the principles and practice are described in detail elsewhere [3].

The grain-to-grain misorientation (and, where applicable, CSL designation) is a broad classification which does not take account of the orientation of the actual interface between grains, which is referred to as the "grain-boundary plane" and can be expressed relative to the lattices of both neighbouring grains [4]. This is an oversimplification, because the crystallography of plane has a large effect on the free volume and hence properties of the boundary [5]. For example, a boundary with a $\Sigma = 3$ misorientation could have irrational boundary planes, whereupon the boundary would not have a particularly low energy, or alternatively, the plane could be indexed as 111 in both grains, whereupon the boundary has a very low energy.

A knowledge of the indices of the boundary plane relative to each interfacing grain allows the boundary to be categorized as follows. Symmetrical tilt boundaries (STB) have the same form of Miller indices on

both sides of the boundary, whereas asymmetrical tilt boundaries (ATB) have different indices. Tilt boundaries are governed by the conditions [4, 5]

$$h_1^2 + k_1^2 + l_1^2 = h_2^2 + k_2^2 + l_2^2 = n\Sigma \text{ (STB) (n is an integer) (1)}$$

$$h_1^2 + k_1^2 + l_1^2/h_2^2 + k_2^2 + l_2^2 = \Sigma^2 \text{ (ATB) (2)}$$

where $h_1k_1l_1$ and $h_2k_2l_2$ are the Miller indices of the boundary plane in each interfacing grain. For a particular low- Σ CSL there are only one or two STBs, but many ATBs. Twist boundaries (TB) have the same form of Miller indices on both sides of the boundary, and the plane normal corresponds to the axis of misorientation for any of the 24 symmetry-related descriptions of the misorientation [4]. Because STBs, ATBs and TBs represent non-random boundary geometries, the implication is that their occurrence is a preferred state for a boundary in a polycrystal. Symmetrical boundary orientations (i.e. same family of planes on both side of the boundary, but not a TB or STB), may also be important.

The $\Sigma = 3$ system has two symmetrical tilt boundaries: 111 planes interfacing from both grains (which will be written as $111/111$) and $112/112$. These are known as the coherent and incoherent twin, respectively. The $\Sigma = 3$ system also has a range of asymmetrical tilt and twist boundaries.

During recent investigations, the boundary-plane orientation of grains in pure nickel have been measured. The data set comprised only grains which abutted the specimen surface during a high-temperature vacuum anneal, such that these boundaries had a far greater freedom of movement than those within the bulk of the material. The main conclusions of those investigations were [6, 7]: (i) most CSL boundaries, except for $\Sigma = 3$ or 9, had irrational planes; (ii) most

$\Sigma = 3$ and 9 boundaries were asymmetrical tilt types; (iii) the free surface had a major effect on the boundary-plane orientation during annealing, allowing it to rotate towards lower energy configurations.

Evidence for the last point was that surface energy minimization criteria allowed boundaries to align nearly perpendicular to the specimen surface during annealing. Measurements of grain-boundary plane crystallography from surface grains in an annealed specimen would therefore not be characteristic of grains in the bulk material.

The purpose of the present work was to investigate the distribution of grain-boundary plane crystallography in pure nickel for grains which are not contiguous with a free surface during annealing, i.e. where boundaries would have far less rotational freedom. This was achieved by annealing in air such that an oxidized layer developed on the specimen surface, thus preventing free ingress of vacancies. $\Sigma = 3$ boundaries are of particular interest because annealed nickel twins heavily, and $\Sigma = 3$ boundaries are often associated with "special" properties.

2. Experimental procedure

Sheet specimens of 99.95% pure nickel were annealed in vacuum for 2 h at 1000 °C followed by 67.5 h at 850 °C in air. The specimens were ground until all evidence of oxidation was removed, then polished and

electrolytically etched in 5% sulphuric acid. The grain misorientations of photographed areas were obtained using EBSD in a scanning electron microscope, and 150 boundaries were analysed to obtain the indices of their planes in addition to their misorientations. For suitable (i.e. non-curved) boundaries, the crystallographic indices of the boundary plane, with respect to both interfacing grains, were obtained using a calibrated serial sectioning technique in conjunction with EBSD. Because this technique is described in full detail elsewhere [4, 8], it will only be summarized here. The technique involves measuring the locations of boundary traces (as revealed by etching) on the specimen surface followed by grinding the etched surface to remove a depth of at least 20 μm . The depth removed is measured accurately by use of SEM images of hardness indents. Because the face angle of a hardness indent is 136°, the depth removal can be calibrated. The locations of the boundary traces after calibrated sectioning (as indicated on Fig. 1) are re-measured and the boundary inclination obtained by simple trigonometry. The boundary inclination is then related to the orientation of each interfacing grain to obtain the crystallographic indices of the boundary plane.

The calibrated sectioning method for the determination of boundary plane indices relies on the boundary being planar throughout the section depth. Moreover, a single set of crystallographic indices



Figure 1 Micrograph showing a typical area where grain-boundary planes have been measured. Positions of boundaries prior to calibrated sectioning are marked with dotted lines. Boundaries that are marked with their idealized Miller indices are all tilt types. All boundaries thus labelled are $\Sigma = 3$ s except for the 211/31,72 ATB which is a $\Sigma = 13$ b.

cannot be quoted for a curved boundary because the boundary surface itself is clearly varying with respect to the lattices of each interfacing grain.

Most boundaries in the sample population were planar throughout the section depth, as illustrated in Fig. 1, except sometimes near the grain-edge (triple) line. Fig. 1 shows the specimen surface after calibrated sectioning, with the "before sectioning" boundary traces superimposed as dotted lines.

3. Results

From spatial information such as that shown in Fig. 1, the inclination of boundary surfaces with respect to the plane of polish can be calculated. The distribution of these inclinations, plotted as the angle between the boundary plane and the specimen surface normal, is shown in Fig. 2. It is evident that the spatial distribution of boundary inclinations for this sample population is random. For comparison the distribution of boundary plane inclinations for grain boundaries in nickel which abutted a free surface during vacuum annealing [6, 7] is also included in Fig. 2. The distribution of these "free surface" boundaries is clearly very different to that of boundaries reported here: boundaries which are perpendicular to the specimen surface predominate in the former, because this is the lowest area position and boundaries have been in contact with a free surface during high-temperature annealing and so were able to rotate. It is clear that the presence of an oxide layer during annealing has greatly reduced the rotational capability of boundaries, because there is no bias towards minimum area inclinations.

The categorization of misorientations in the sample population is as follows:

$$\Sigma = 3 \text{ 61\%}$$

$$\Sigma = 9 \text{ 6\%}$$

Other CSLs and low-angle boundaries 9%

General boundaries 24%.

Not every boundary having a general (random) misorientation was chosen for boundary plane analysis because firstly general boundaries were more likely than CSLs (especially $\Sigma = 3$ s) to be curved, and secondly, in agreement with previous observations [4], all the general boundaries which were selected for full analysis had irrational boundary-plane indices.

Table I gives details of the crystallographic analysis for CSL boundaries (excluding $\Sigma = 3$ s) for those cases where the boundary inclination could be measured. The data recorded in Table I are the Σ value, relative deviation from the exact CSL, Miller indices of the boundary plane in each interfacing lattice plus angular deviation from the exact plane listed, and boundary type (asymmetrical tilt, twist, irrational planes). Most of the experimental plane analyses and the discussion which follows refers to the $\Sigma = 3$ set because these were by far the most numerous in the sample population (61%). The $\Sigma = 3$ data are presented in Table II,

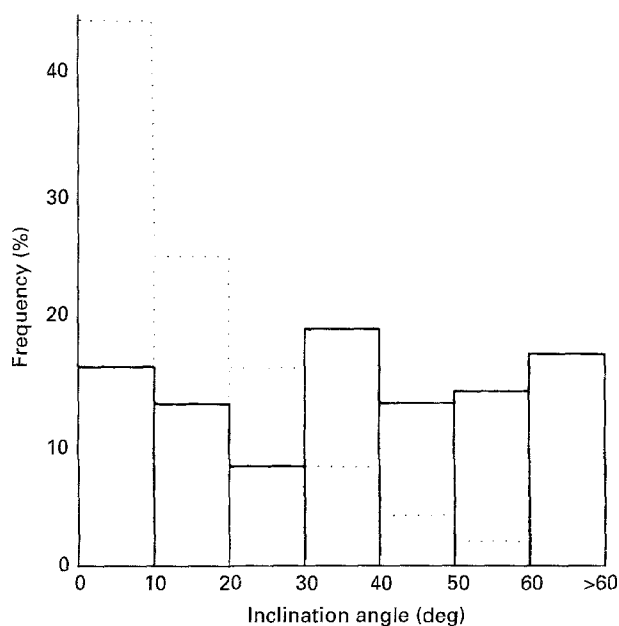


Figure 2 Frequency distribution of grain-boundary inclinations, expressed as the angle between the grain-boundary surface and the specimen surface normal, for the entire sample population of boundaries. The inclination frequency distribution of boundaries which had abutted a specimen surface during annealing is also included, for comparison, as a dotted outline.

TABLE I Details of grain-boundary crystallography for Σ boundaries, excluding $\Sigma = 3$

Σ	Planes/deviation	Type
7	Irrational	-
9	2 2 1/21, 14, 7 0.8° 5.6°	ATB
9	3 2 1/3 2 1 1.5° 0.9°	TB
9	Irrational	-
9	-	-
9	Irrational	-
9	3 1 1/3 1 1 6.7° 6.3°	TB
9	2 1 1/7 2 1 2.3° 1.8°	ATB
13b	2 1 1/31, 7, 2 6.5° 2.7°	ATB
13b	2 2 1/29, 22, 14 3.1° 5.2°	ATB
19a	2 1 1/3 1 1 2.4° 4.4°	-
25b	9 5 1/25, 13, 13 0.9° 1.5°	ATB
25b	Irrational	-
27a	-	-
27a	Irrational	-

classified as proportions according to the Miller indices of the boundary planes and also the boundary type.

4. Discussion

It is evident from examination of the experimental results in Tables I and II that there are well-defined trends in the distribution of boundary types. In particular, most $\Sigma = 3$ s are either STBs or ATBs with low

TABLE II Details of grain-boundary crystallography for $\Sigma = 3$ boundaries

Planes	Type	% (of $\Sigma = 3s$)	Angle from STB
111/111	ST	28.0	0
23, 17, 17/775	AT	14.1	8.5
332/10, 77	AT	4.3	10.0
774/855	AT	2.5	13.3
221/744	AT	17.5	15.8
211/552	AT	7.2	19.5
522/441	AT	0	25.2
331/771	AT	6.3	29.5
110/411	AT	2.5	35.3
881/11, 22	AT	0	40.3
551/711	AT	1.3	43.3
772/10, 11	AT	2.5	46.7
221/100	AT	0	54.7
775/11, 11	AT	0	62.1
111/511	AT	0	70.5
544/722	AT	0	76.7
322/11, 44	AT	0	82.0
11, 77/13, 55	AT	0	83.3
211/211	ST	0	90
310/754	AT	3.9	–
851			
210/210	T	2.8	–
Other hkl/hkl	–	3.0	–
Irrational	–	3.8	–

Miller indices. By contrast, for CSLs other than $\Sigma = 3$ boundary planes are either irrational or ATBs with high Miller indices in one of the interfacing grains and furthermore STBs are not observed. These observations agree with those made previously for CSL (non $\Sigma = 3$) grain boundaries abutting free surfaces [6, 7]. A boundary plane having irrational indices in both grains would have a high free volume. Free volume correlates with boundary energy [9], and so such boundaries would, in turn, have high energies. ATBs with high Miller indices may also have relatively high free volume and thus not have low energy.

Early interpretations of the CSL model envisaged that the boundary plane would follow the lowest energy path through the lattice, which is usually the STB [10]. Furthermore, “sphere-on-plate” investigations have demonstrated that the CSL is a preferred state for two adjacent lattices where one has complete rotational freedom [11] (although the orientation of the boundary plane in such experiments has not been reported). The present results show that in polycrystals the physical limitations of grain coherence are such that the lowest energy planes in a CSL are not achieved. This calls into question whether or not all CSLs are “special” with regard to properties. The inference from the present and recent observations is that CSLs in polycrystals are not always associated with special properties [12], although fabricated CSL bicrystals with a symmetrical boundary plane frequently do show special properties [13].

Turning now to the data for $\Sigma = 3s$, Table II shows that there is a spread of plane types for $\Sigma = 3$ boundaries: a small proportion (<5% each) are irrational planes, symmetrical boundaries and TBs, 28% are 111/111 STBs and the great majority are ATBs. There are two observations on the ATB class which

are particularly noteworthy: firstly whilst the proportion of incoherent twins (ATBs) is high (nearly two-thirds of $\Sigma = 3s$), the 211/211 STB twin is not observed and secondly all the $\Sigma = 3$ tilt boundaries (except 6% which are 310/ hkl ATBs) are on the 110 zone.

The significance of $\Sigma = 3$ tilt boundaries on the 110 zone is that they have low energies, because their structure is composed of a mixture of units from the 111/111 and 211/211 STBs [14]. Computer simulations and experiment have shown that the energy increases monotonically, starting from a very low value of 0.01 J m^{-2} for the 111/111 STB, up to 70° away from the 111/111 STB along the 110 zone. After a small energy dip (which is explained elsewhere [14]) the energy continues to increase up to 0.54 J m^{-2} for the 211/211 STB which is 90° from 111/111 on the 110 zone. Consequently, the 211/211 STB has a higher energy than “incoherent twins” such as 221/744 or 011/411, for example, which are 16° and 19° from 111/111, respectively, and have energies of 0.22 and 0.41 J m^{-2} . Hence the ATBs which are observed have largely been selected on the basis of energy minimization, since column 3 of Table II shows that the $\Sigma = 3$ boundary crystallographies are biased towards small angles away from 111/111.

Table II also includes a selection of other possible plane combinations and their angular deviation from 111/111 to illustrate that those ATBs which deviate by large angles from 111/111 are not observed. On an atomic scale, boundaries on the 110 zone correspond to the gradual incorporation of structural units associated with the 211/211 STB into a boundary composed of structural units from the 111/111 STB, with increasing deviation from 111/111 [14]. At the limits, the 111/111 and 211/211 STBs are both composed of a single structural unit type.

The identity of boundary planes for $\Sigma = 3s$ is not predictable from their morphology in a two-dimensional section, as illustrated in Fig. 1 where several types of $\Sigma = 3$ are present. Furthermore, the angular mismatch of the misorientation from the exact $\Sigma = 3$ also does not distinguish between boundary planes, because almost all the reported $\Sigma = 3s$ have small angular deviations from the CSL reference misorientation. Fig. 3 illustrates this trend by showing the relative deviation from the $\Sigma = 3$ (where the relative deviation is between 0 and 1, with 1 corresponding to 8.66° , the maximum deviation according to the Brandon criterion [10]) for all the twins grouped according to boundary type. Most of the twins are within 0.3 of the exact CSL matching, and 111/111 STBs are no closer to exact CSL matching than other $\Sigma = 3s$. An exception is four $\Sigma = 3s$, shown on Fig. 3, which have irrational planes and higher relative deviations than most of the STBs or ATBs. These observations highlight the importance of having a knowledge of the grain-boundary plane crystallography in addition to the misorientation, because the free volume and hence properties of boundaries may be inferred from the boundary-plane type, and this is not known from the misorientation alone.

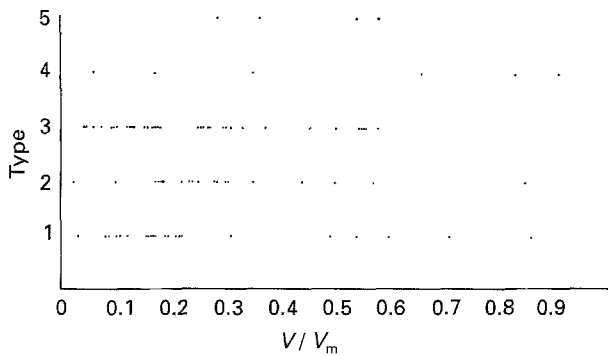


Figure 3 Distribution of $\Sigma = 3$ types according to the relative deviation from exact CSL matching, expressed as V/V_m where V is the experimentally measured deviation and V_m is the deviation limit according to the Brandon criterion, i.e. 8.66° . The $\Sigma = 3$ types are: 1, 111/111 STB; 2, 23, 17, 17/775 and 3 3 2/10, 77 "near STBs"; 3, ATBs on the 110 zone and TBs; 4, other ATBs; 5, irrational planes.

A further trend in the $\Sigma = 3$ data is the tendency for certain ATB twins to occur in adjacent or nearby grains as illustrated in Fig. 1 for 411/110 and 722/10, 11 ATBs. This is the only area in the sample population where these particular ATBs were observed. The reasons for this local clustering of plane types is as yet obscure, because it does not appear to relate directly to the grain orientation.

Each exact ATB position is a reference structure in the same way that the exact CSL is a reference structure for misorientation. The implication is that each boundary reference structure is an energy minimum which the boundary will try to attain. For $\Sigma = 3$ boundaries on the 110 zone, energy differences between local minima are small [14], giving the effect of an "energy valley" for boundaries on this zone. The energies of boundaries on this zone range from 0.01 – 0.61 J m^{-2} , which compares to a value of approximately 1 J m^{-2} for a totally disordered, general boundary.

The average angle which a measured plane in the $\Sigma = 3$ data set deviates from the reference plane is 3.5° . This compares to an estimated resolution of the measurement technique of approximately 2.5° [4, 8]. However, it is important to note that mismatches from the exact plane are systematic in the sense that the deviation tends to be similar in magnitude on both sides of the boundary. Fig. 4 provides quantification of these statements: it shows a frequency distribution of the difference in angular mismatch between pairs of interfacing grains. For example, one particular $\Sigma = 3$ grain boundary was found to have a boundary plane which was indexed in each grain as 0.665, 0.532, 0.525 and 0.639, 0.604, 0.477. These indices are 2.1° and 2.2° from 23, 17, 17 and 775, respectively, which gives an angular mismatch difference for indexing in each grain of 0.1° .

Fig. 4 indicates that most of the boundary-plane index pairs (i.e. the same boundary indexed in both interfacing grains) differed by less than 2° , and nearly half the boundaries (47%) differed by less than 1° . If the measured mismatch from the exact plane for an STB or ATB were due to experimental error alone, the

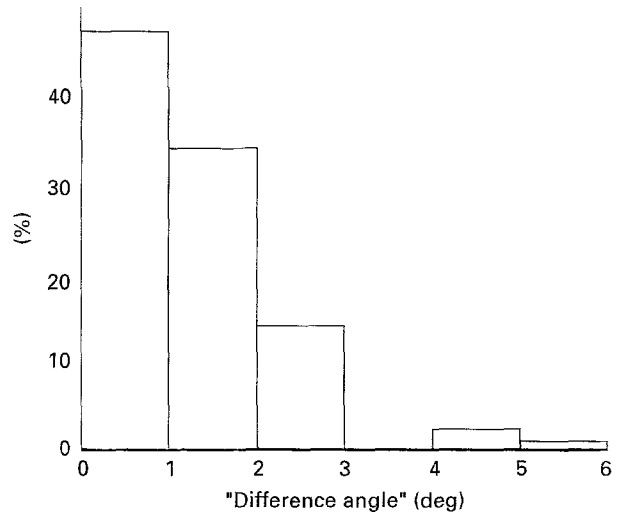


Figure 4 Distribution of "difference angles" between the two interfacing boundary plane indices for $\Sigma = 3s$, where the "difference angle" is the difference between the mismatch of each experimentally measured plane from the exact Miller indices of the reference structure.

angular difference within boundary-plane index pairs would be uncorrelated pairwise.

The heat-treatment schedule for this experiment, 850°C for 67.5 h, was chosen to be sufficiently low that grain growth was not activated, yet there was sufficient thermal energy to promote changes in the inclinations of twin boundaries (and, to a lesser extent, grain boundaries) so as to move towards nearby lower energy reference structures, usually an ATB, wherever possible. It is suggested that the experimental results for the orientations of twin boundaries are reflecting this trend.

There has been little previous work on polycrystals with which to compare the present data. Two previous investigations of grain-boundary plane geometries in copper [15] and nickel [6] have shown that most of the $\Sigma = 3$ boundaries are ATBs and that some of these are on the 110 zone. However, for both previous sets of data there is a weaker correlation of incoherent twins with proximity to the 111/111 STB than that reported here. One reason for this is that both previous data sets are strongly influenced by free surfaces: boundaries in the nickel sample population abutted the surface of a specimen annealed for 2 h at 1000°C [6] and boundaries in the copper sample population were from thin-sheet specimens annealed at 1000°C for 70–200 h [15], both in inert atmospheres. It was apparent from Fig. 2 that the inclinations of boundaries abutting a free surface during annealing are very different from those separated from the surface by the oxide layer, and the orientation of the boundary plane will be likewise affected.

One way to view the deviation of an experimental boundary from the reference structure is as a superimposed low-angle boundary which has both tilt and twist components. Using an experimental $\Sigma = 3$ boundary which is near a 221/744 ATB (3.6° from each) as an example, the misorientation parameters and tilt/twist components for both the measured and

reference structures are:

measured components:

misorientation angle/axis = 72.7°/0.682 0.731 0.011

tilt angle/axis = 72.4°/0.749 0.661 0.035

twist angle/axis = 7.1°/0.393 0.487 0.783

reference components:

misorientation angle/axis = tilt angle/axis

= 70.5°/1 1 0

twist angle/axis = 0°/4 4 7

which gives tilt and twist deviations of 4.1° and 5.7°, respectively, of the measured data from the reference structure. These deviations are accommodated by edge and screw dislocations, which may be localized into discrete entities such as steps or ledges at the boundary, or delocalized. Equivalently, the mismatch may be thought of as being accommodated by distortions in the polyhedra which form the structural units of the boundary. It is quite likely that the identity of the grain-boundary plane on a macroscopic scale is an over simplification of the actual structure on an atomic level [16]: probably the microscopic structure consists of ledges of well-fitting structural units interspersed with steps or other (distorted) structural units, as was originally envisaged as a "boundary coincidence" model [17].

Finally, it is apparent that perfectly coherent twins occur less frequently than is usually assumed; those boundaries which are close to 23, 17, 17/775 can probably be thought of as "off" STBs rather than ATBs. For these "off coherent" twins the arrangement of 1 1 1/1 1 1 and 2 1 1/2 1 1 units on an atomic level may be such that large groups of 1 1 1/1 1 1 units are contiguous in the boundary plane, interspersed with single 2 1 1/2 1 1 units.

5. Conclusions

1. In a polycrystalline nickel specimen, CSLs (other than $\Sigma = 3$) either have irrational boundary planes or are ATBs with high Miller indices. STBs were not

observed. The inference is that CSL designations from misorientations alone are not necessarily associated with low free volume interfaces and thus special properties.

2. Half of the $\Sigma = 3$ boundaries were ATBs on the 1 1 0 zone, and correlate with proximity to the 1 1 1/1 1 1 STB. The 2 1 1/2 1 1 "incoherent twin" was not observed. These results were explained on the basis of a low-energy criterion.

3. The type of $\Sigma = 3$ boundary – STB, ATB, TB or irrational planes – cannot be distinguished either by morphology or proximity to the exact $\Sigma = 3$ misorientation.

References

1. J. FURLEY and V. RANDLE, *Mater. Sci. Technol.* **7** (1991) 12.
2. D. P. FIELD and B. L. ADAMS, *Acta Metall. Mater.* **40** (1992) 1145.
3. V. RANDLE, "Microtexture determination and its applications" (Institute of Materials, London, 1992).
4. *Idem*, "The measurement of grain boundary geometry" (Institute of Physics, Bristol, 1993).
5. D. WOLF and J. F. LUTSKO, *Z. Kristallogr.* **189** (1989) 239.
6. V. RANDLE, *Acta Crystallogr.* **A50** (1994) 588.
7. *Idem*, *Acta Metall. Mater.* **42** (1994) 1769.
8. *Idem*, *Mater. Char.*, in press.
9. S. C. MEHTA and D. A. SMITH, in "International symposium on grain boundary engineering", edited by U. Erb and G. Palumbo (Canadian Institute of Mining, Metals and Petrology", Montreal, 1993) p. 1.
10. D. G. BRANDON, *Acta Metall.* **14** (1966) 1479.
11. G. HERRMANN, H. GLEITER and G. BARO, *ibid.* **24** (1976) 353.
12. S. I. WRIGHT and F. HEIDELBACH, *Mater. Sci. Forum* **157–162** (1994) 1313.
13. G. PALUMBO and K. T. AUST, in "Materials interfaces: atomic level structure and properties", edited by D. Wolf and S. Yip (Chapman and Hall, London, 1992) p. 190.
14. U. WOLF, F. ERNST, T. MUSCHIK, M. W. FINNIS and H. F. FISCHMEISTER, *Philos. Mag. A* **66** (1992) 991.
15. R. OMAR, PhD thesis, University of Warwick, UK (1987).
16. K. L. MERKLE and D. WOLF, *Philos. Mag. A* **65** (1992) 513.
17. G. H. BISHOP and B. CHALMERS, *Scripta Metall.* **2** (1968) 133.

Received 15 February
and accepted 22 March 1995